Journal of
Composites Science

MDPI

Article

Synthesis and Wear Behaviour Analysis of SiC- and Rice Husk Ash-Based Aluminium Metal Matrix Composites

Sameen Mustafa [1,*], Julfikar Haider [2,*], Paolo Matteis [3] and Qasim Murtaza [4]

[1] Faculty of Engineering, Free University of Bozen-Bolzano, 39100 Bolzano, Italy
[2] Department of Engineering, Manchester Metropolitan University, Manchester M1 5GD, UK
[3] Department of Applied Science and Technology, Politecnico di Torino, 10129 Turin, Italy; paolo.matteis@polito.it
[4] Department of Mechanical Engineering, Delhi Technological University, Delhi 110042, India; qasimmurtaza@gmail.com
* Correspondence: smustafa@unibz.it (S.M.); j.haider@mmu.ac.uk (J.H.)

Abstract: Research efforts seek to develop aluminium alloy composites to enhance the poor tribological performance of aluminium alloy base matrix. In this research, a hybrid metal matrix composite (HMMC) was developed by reinforcing an aluminium alloy (AA8011) with SiC and rice husk ash (RHA) using a stir casting technique. RHA was prepared by the cracking of rice husk, which is abundantly available in the Indian subcontinent. The samples were cast by keeping the amount of RHA constant at 2.5 wt.% and varying the amount of SiC from 0.0 wt.% to 8 wt.%. The samples were machined to manufacture pins for wear tests (at ambient temperature, 100 °C, and 200 °C) and hardness measurement. The microstructures of the cast samples were analysed using an X-ray diffractometer (XRD) and a scanning electron microscope (SEM), along with energy-dispersive X-ray spectroscopy (EDS). It was observed that the composites with greater reinforcement of SiC exhibited improved hardness and wear resistance, but the coefficient of friction increased with the addition of RHA and SiC, and the wear performance deteriorated with an increase in the operating temperature. The contribution of RHA alone to the improvement in wear performance was marginal compared to the pure alloy. It was also confirmed that the reinforced composites could be a better option for automotive applications to replace aluminium alloys.

Keywords: metal matrix composite (MMC); SiC; rice husk ash (RHA); stir casting; wear

Citation: Mustafa, S.; Haider, J.; Matteis, P.; Murtaza, Q. Synthesis and Wear Behaviour Analysis of SiC- and Rice Husk Ash-Based Aluminium Metal Matrix Composites. *J. Compos. Sci.* **2023**, *7*, 394. https://doi.org/10.3390/jcs7090394

Academic Editor: Francesco Tornabene

Received: 17 August 2023
Revised: 6 September 2023
Accepted: 13 September 2023
Published: 15 September 2023

1. Introduction

Composite materials amount to approximately 12.5% of the overall industry of engineering materials [1]. Composites have replaced bronze and cast-iron, as they exhibit low density and higher mechanical strength compared to these materials. Despite these enhanced material properties, composites are extensively being researched to enhance their low wear and seizure resistance [2]. Over the past decades, numerous studies have explored and reported on the wear behaviour of composites. In this study, the focus is on investigating the wear behaviour of aluminium metal matrix composites (AMMC) reinforced with SiC and rice husk ash (RHA).

Aluminium and aluminium alloys are finding increasing applications in various technical fields. They are employed in aviation, aerospace, military, automotive, and electronic industries. To improve the tribological and mechanical characteristics of aluminium alloys, different reinforcements are added, and corresponding composites are formed [3,4]. AMMCs reinforced with materials such as SiC, B_4C, and other ceramics are increasingly being utilised in the automotive, aerospace, underwater, and transportation industries. The addition of reinforcements such as ceramics and ash improve tribological and mechanical properties like strength, stiffness, impact, wear, and abrasion resistance. In recent years, the addition of fillers (graphite, fly ash, material fibres from wheat husk ash, and jute

ash) to AMMCs is being studied to obtain good toughness levels [5]. If the base metal alloy is mixed with reinforcing particles such as SiC or B_4C and fibre particles such as ash, the resulting product is called a hybrid metal matrix composite (HMMC) [6]. For applications in the automotive and aerospace industries, lightweight and high-performance materials are required. The lightweight material is produced by developing composites with hard reinforcement particulates in the matrix of soft material [7]. Singh et al. reported that, for application in the automobile, aerospace, and aircraft industries, lightweight and high-performance materials are required [7].

The addition of SiC can increase both the mechanical strength and the wear performance of AMMCs. Additionally, it has been reported that hybrid composites exhibit superior wear properties of worn surfaces as compared to pure Al alloys [8]. SiC particles possess excellent compatibility with aluminium matrices, and they can be obtained at a low cost. A major application of AMMCs involves moving and sliding parts. Therefore, the investigation of the tribological properties of these materials is of significant importance for us to determine the behaviour of composite materials during service application [9]. The applied load and sliding distance during the wear test affects the coefficient of friction (COF) to a greater extent, and an increased silicon carbide content offers better wear resistance in the HMMC [10]. It has been found that the wear resistance of the HMMC is higher than that of the corresponding base alloy. The addition of hard reinforcements, such as B_4C and fly ash, shows a greater improvement in wear performance [11,12].

AA8011 is a type of AMMC that exhibits higher ductility and malleability than most of the other AMMCs [13]. It contains a rare mix of desirable properties such as low weight, low maintenance, and good corrosion resistance. Studies are conducted to enhance the strength of AA8011 by reinforcing it with ceramic particles to make it more durable and increase the scope of its application [14]. Furthermore, it has been observed that the wear decreases when the amount of reinforcement element is increased [15,16]. In addition, it has been determined that the COF increases with the sliding velocity [17].

The addition of ceramics such as titanium diboride can significantly improve the wear behaviour of AMMCs due to the formation of a mechanically mixed layer of Fe_2O_3. [17]. Karthikumar et al. prepared Aluminium 8011 MMC by stir casting using TiB_2 as a reinforcement. The study concluded that the maximum hardness of 55.03% was exhibited in the case of 8% by weight of TiB_2 reinforcement. Also, maximum % elongation was found in the case of 4% by weight of TiB_2 [18].

Studies have reported that the reinforcement of AMMCs with Al_2O_3 increases the wear resistance of the HMMC as compared to the corresponding matrix material, AL-6061 [19]. When the operating temperature increases, the wear rate decreases constantly with the increase in sliding velocity. Further, the increase in the reinforcement volume fraction increases the wear resistance of the composites [20,21].

According to a study, for every ton of paddy processed, an average mill produces 200 kg of rice husk and 40 kg of RHA [22]. Thus, the total amount of rice husk produced in India is estimated to be about 24 million tons, while the RHA production is estimated to be around 4.8 million tons per year. Since rice is a diet staple in India, the choice of a strengthening particle such as RHA provides a possible sustainable option for countries like India. This could help with utilising the waste obtained from rice harvesting.

Although research is being carried out to study the enhancement of the properties of AA8011 MMC, the aspect of characterising the physical wear of AA8011 at different temperatures and its surface morphology has not often been studied yet in terms of the wear on the AMMC. The exploration of modifying Al alloys with two different kinds of fillers, i.e., typical ceramic (SiC) particles and plant-based waste (RHA), might be of engineering significance. This study explores the wear behaviour of an HMMC (AA8011 reinforced with SiC and RHA) through experimental testing. The HMMC samples were prepared using the stir casting technique, which is the most suited for producing reinforced AMMC.

The principal contribution of this research lies in its pioneering utilisation of RHA as a reinforcement material, which not only demonstrates its viability for enhancing the tribological properties of aluminium alloy composites, but also underscores its potential to significantly reduce the waste generated from rice harvesting. In this context, the most efficient utilisation of natural resources can be pursued [23]. Additionally, the development of a hybrid composite, blending RHA and SiC with an aluminium alloy base matrix, allows for the prospect of achieving a well-balanced amalgamation of mechanical properties. This approach, involving systematic variation in SiC content, facilitates a meticulous examination of its impact on the composite's characteristics. This could substantially contribute to mitigating the ecological footprint by valorising an abundant agricultural by-product. Consequently, the dissemination of this research through publication stands to advance the body of knowledge in the field of materials science and engineering, with far-reaching implications for the development of sustainable, high-performance composite materials and reducing agricultural waste stemming from rice harvesting practices.

2. Materials and Methods

2.1. Preparation of Cast MMC Samples

To prepare the HMMC, first, the aluminium alloy was melted in a stir casting furnace and the blended powder mix (SiC and RHA) was fed into the melt. The stir casting process was selected to produce metal matrix composites due to its inherent advantages, despite its drawbacks relative to alternative casting techniques. This choice was primarily driven by factors such as cost-effectiveness, material flexibility, and the ability to achieve homogeneous mixing. While it exhibits limitations such as potential porosity and limited control over reinforcement distribution, these drawbacks can often be managed effectively, making stir casting a pragmatic choice in scenarios where cost efficiency, rapid prototyping, and ease of implementation are paramount.

After thorough mixing, the melt was poured into a cylindrical cast-iron die to prepare samples. Freshly obtained rice husk contains a large amount of moisture and oil; thus, it does not burn, but chars into black, brittle material when torched. Therefore, to prepare a fine RHA powder, the rice husk was charred overnight using the indigenous method. The burnt husk was then milled to a fine powder using a ball mill. SEM and EDS of the milled ash were then carried out to identify the powder's morphology and chemical composition.

Commercially available SiC powder was used in the experiment. To obtain a homogenous mix of RHA and SiC, the milled ash and SiC powder were blended in the ball mill for at least 30 min. Before blending, SiC powder was carefully measured using a precision balance according to the different weight percentages required for the samples. The measurement of RHA was kept constant at 2.5% by weight for each cast sample. The samples' nomenclature and their respective compositions are given in Table 1.

Table 1. Nomenclature and composition of samples.

Sample Group Number	Sample ID	wt.% of AA-8011	wt.% of SiC	wt.% of RHA
S1	8SiC/2.5RHA	89.5	8	2.5
S2	6SiC/2.5RHA	91.5	6	2.5
S3	4SiC/2.5RHA	93.5	4	2.5
S4	2SiC/2.5RHA	95.5	2	2.5
S5	0SiC/2.5RHA	97.5	0	2.5
S6	0SiC/0RHA	100	0	0

The work-hardened AA8011 alloy was purchased in the form of sheets with a composition of 98.7% Al, 0.7% Fe, and 0.6% Si. The sheets were cut into smaller plates, each weighing around 20 g. Looking at the size of the die, the aluminium alloy required to fill

the die was calculated as approximately 380 g. The precise weight of the alloy was placed into the crucible by carefully choosing the correct number of smaller plates. The alloy was subsequently melted in a furnace, maintaining a constant temperature of 900 °C for a minimum of 20 min. In parallel, the RHA/SiC mixture was preheated in a muffle furnace at 350 °C. This step served two purposes: ensuring the complete dryness of the mixture and minimizing the temperature disparity between the mix and the molten metal.

The heated powder mix was then fed into the stir casting furnace, and stirring was carried out using a mechanical stirrer for at least 20 min. Since the experimentation was carried out during the winter, with ambient temperatures being lower than 20 °C, the die had to be pre-heated to minimise the directional solidification and heat transfer during the casting process. The final sample was obtained as a solid cylinder. A total of 18 samples were prepared, with 3 samples for each material group.

The cast samples were cut into smaller parts using a hacksaw. The cut pieces were then precision-turned on a universal lathe in order to reach a final diameter value of 6 ± 0.05 mm, and the lengths of the pins were kept at 50 ± 2 mm. It is to be noted that the pins needed to be prepared through conventional machining. This was due to the fact that blow holes are very common in gravity-cast samples, and that the in-fusion of non-conducting particles of ceramic and ash make it almost impossible to cut the samples using a wire-cut EDM process.

2.2. Characterisation of Samples

The castings were cut into small discs to measure their hardnesses by a Rockwell C Hardness (RHN) tester. For each sample, hardness was measured at 5 different points, and the average for each sample was recorded. A load of 100 kgf and an indentation ball diameter of approximately 1.6 mm were chosen for the hardness measurements. For SEM and EDS analysis (EDS, Jeol, JSM-6510LV, Tokyo, Japan), the cast samples were further cut into small, plate-like pieces, and one surface of each sample was ground to a fine finish. The structural analysis of the samples was performed on an XRD machine (Shimadzu LabX, Kyoto, Japan), which had a monochromatic Cu source of Kα wavelength of 1.540 Å. The measurement conditions for XRD were as follows: voltage = 40.0 (kV), current = 30.0 (mA), scan range = 10.00–80.00 (deg), scan speed = 6.00 (deg/min), and sampling pitch = 0.02 (deg). The scanning time for each sample was around 11 min. The diffraction patterns were plotted using OriginPro software version 9.7.

2.3. Wear Test Procedure

The dry friction wear test was conducted using a pin-on-disc tribometer able to conduct tests at elevated temperatures, either by heating the pin or the disc. The selection of a pin-on-disc tribometer for the wear analysis of aluminium composites was underpinned by its capacity to closely emulate real-world wear conditions, affording a comprehensive understanding of material performance. This apparatus offers meticulous control over experimental parameters, encompassing load, sliding speed, and environmental factors, thus ensuring the reproducibility of wear tests and facilitating the systematic evaluation of diverse composite formulations [24]. Moreover, pin-on-disc tribometers furnish quantitative data on wear rates and coefficients of friction, crucial for the rigorous assessment of aluminium composites and their suitability for specific industrial contexts [25,26]. The examination of worn surfaces and wear debris enables the discernment of wear mechanisms, thereby guiding material enhancement endeavours. Furthermore, the adaptability of these tribometers to varying materials and conditions, coupled with their cost-effectiveness and expeditious testing capabilities, renders them a pragmatic choice for elucidating the tribological behaviour of aluminium composites and advancing their performance characteristics in numerous engineering applications [8]. In this case, the pins were heated at different temperatures and the disc temperature was kept constant. The pin was inserted into the holder, which was heated by an electrical coil, and the temperature of the pin was measured by a thermocouple attached to it. The friction pair was chosen to be the

AA-8011 HMMC pin and high carbon EN-31 (100Cr6) steel disc. The disc material had a much greater hardness level than the HMMC. This type of coupling was chosen intentionally to observe the wear behaviour of the casted samples only. The wear test parameters were kept constant during each test, with a sliding speed of 300 rpm, a track diameter of 80 mm, and an applied load of 30 N. Each set of pins was tested at varying temperatures of 22 °C (ambient), 100 °C, and 200 °C. The choice of this experimental set-up bears significant relevance to several industrial domains, including the automotive, aerospace, and manufacturing sectors. Within the automotive industry, it serves as a valuable tool for assessing the wear and friction characteristics of composite materials like Al/SiC/Gr under conditions that simulate the temperature fluctuations encountered by engine components during operation [12,27]. Such insights are instrumental in the development of lightweight and high-performance materials for applications such as pistons and cylinder liners. Similarly, in the aerospace sector, this tribomechanical system aids in evaluating the performances of composite materials in critical components subjected to diverse temperature conditions, ensuring the safety and reliability of the aerospace systems [3,19]. These references underscore the significance of studying the tribological behaviour of the composite materials under fluctuating temperature conditions across different industrial applications. The disc was not heated, and its temperature was kept constant at 22 ± 2 °C. A total of 18 samples (3 samples from each group) were tested on the tribometer. Each composition was tested at three different temperatures. The results for frictional force (N) and sliding distance (m) were recorded automatically by the tribometer's software. The pins were also weighed (using a precision balance with an accuracy of 0.0001 g) before and after performing the wear tests, and the weight differences were recorded in order to calculate the volumetric wear.

3. Results and Discussion

3.1. Microstructure and Composition

From the SEM observation, it could be inferred that the RHA was a homogenous mixture of bimodal particle size, as shown in Figure 1a. The bigger particles are marked with red, and the smaller ones with green. Particle size was measured in accordance with the scale shown in SEM micrographs, and then mean value was computed. Smaller ash particles adhered to bigger particles with homogenous blending. The smaller particles varied in size from 7 µm to 15.6 µm, while the larger particle sizes were in the range of 46.8 µm to 156.2 µm.

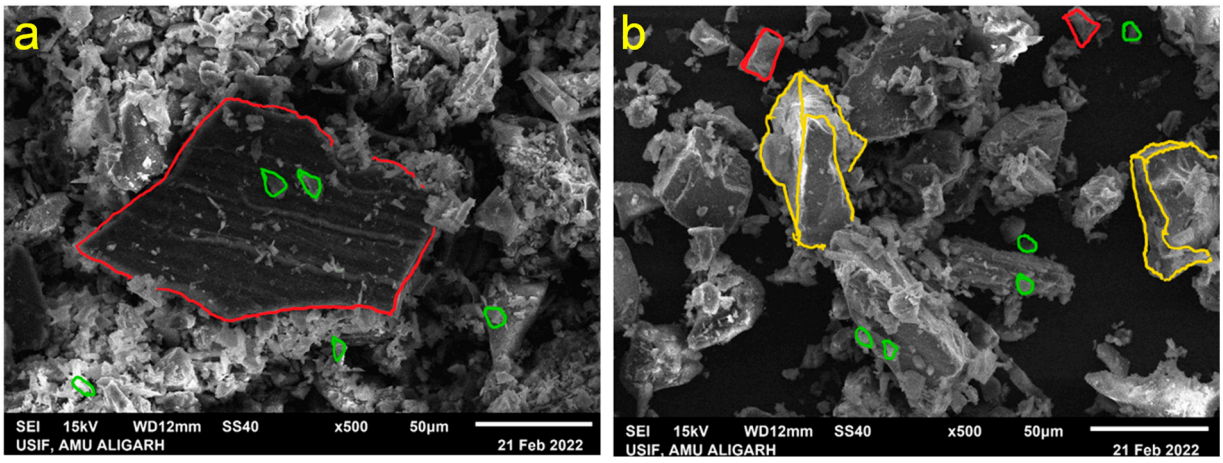

Figure 1. SEM images of (**a**) ash and (**b**) the ash and SiC powder mix at ×500.

An SEM micrograph of the powder mix (RHA+SiC) is shown in Figure 1b. It was clearly seen that the wedge-like particles (SiC) were uniformly dispersed, along with other irregularly shaped particles, as desirable. The abrasive particles can be seen marked in

yellow, while the larger- and smaller-sized ash particles are marked with red and green, respectively. The SiC particles were clearly distinguishable from the RHA particles based on size and shape.

The EDS spectra of the powders, as well as the metal samples, were analysed. The specimens were tested for all the possible elements, and no peaks were omitted. Figure 2 shows the spectrum and composition chart of the RHA. Similarly, the spectra for the other samples were also obtained. The results obtained for the powdered RHA and powder mix are summarised in Table 2. Higher percentages of silicon and carbon in the powder mix compared to the RHA indicated the presence of SiC. This supports the findings in the SEM images.

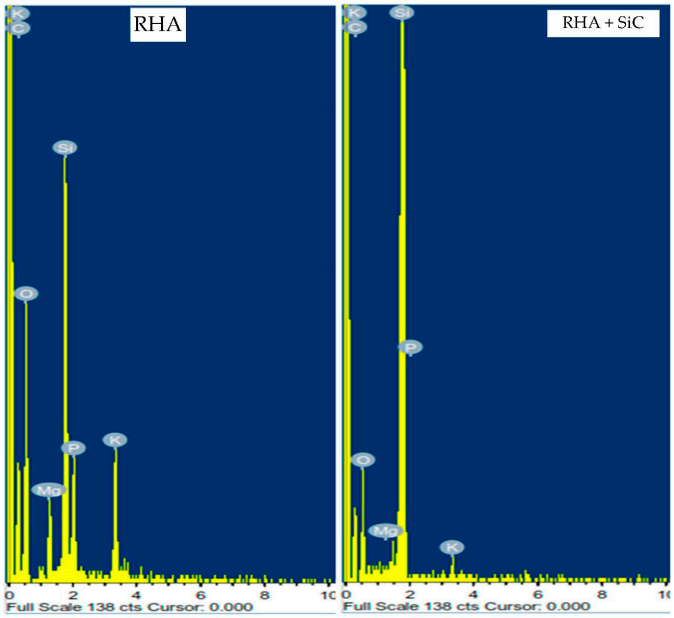

Figure 2. EDS elemental distributions for RHA and RHA+SiC powder mix.

Table 2. EDS compositions of pure RHA and a mix of RHA+SiC powders.

Elements	Weight Percentage	
	RHA	**RHA+SiC**
C	24.50	27.09
O	48.61	21.54
Mg	2.63	0.07
Si	13.17	50.30
P	4.88	0.14
K	6.20	0.87

A small axial cross-section from the mostly highly reinforced sample was mounted, ground, and polished, then observed under an optical microscope (Figure 3). It can easily be observed that the hybrid composites contained two phases. One phase is light grey in colour, and the other phase can be seen as dark grey dendritic phases dispersed throughout the matrix. These two phases can indicate the base metal matrix and Si dissolved in HMMC, respectively. To support this evidence, the EDS spectrum of the respective composite was sufficient, as it showed a peak of elemental Si. During preheating and mixing in the molten MMC, silica present in the ash might have turned into silicon and dissolved into the metal matrix to form a second phase of Si in Al. On the other hand, inclusions of SiC particles can be seen as very prominent, irregularly shaped dark grey particles embedded in large

groups or pockets throughout the sample. The ash was amorphous; therefore, it was more likely to dissolve in the liquid aluminium than the SiC powder. However, the dissolving of some SiC could not be completely ruled out.

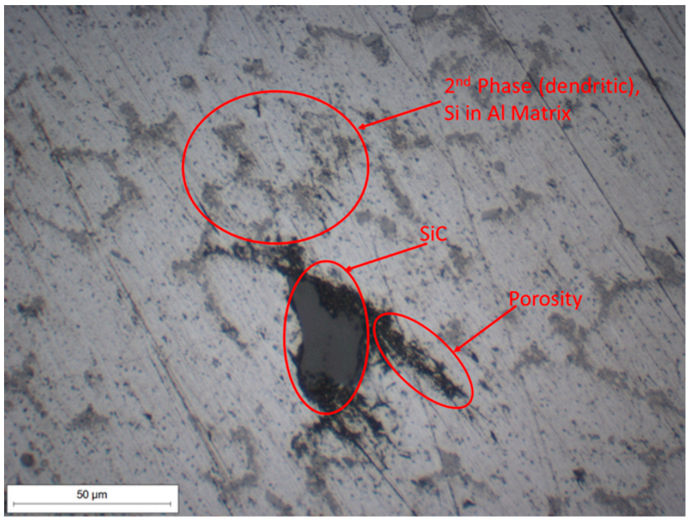

Figure 3. Axial cross-section of 8SiC/2.5RHA, observed under a microscope.

3.2. XRD Analysis

The spectrum of RHA shown in Figure 4 resembles the spectrum of an amorphous material, and is a typical graph of amorphous silica with no pronounced peaks [28,29]. The XRD spectra of pure AA8011, HMMC with 4% SiC reinforcement, and powder mix are shown together in Figure 5. It was observed that the spectrum of pure Al alloy (S6) was in accordance with JCPDS card no. 65-2869 [30], showing Al peaks. The spectrum of the powder mix (RHA+SiC) was also in accordance with JCPDS card no. 29-1129, with peaks of SiC. The HMMC spectrum showed additional small peaks compared to the spectrum of the original Al alloy. These small peaks in the S3 spectrum were, however, not present in the RHA+SiC spectrum. If the weak peaks in S3 represented SiC phase coming from the powders, much higher peaks should have been found in the very same angles in the RHA+SiC spectrum, but they were not present. This indicated that the small peaks could come from the silicon phase identified in the optical microscopic images, while the amount of the SiC phase is probably too low to be found by XRD. This is certainly an interesting observation and requires further investigation.

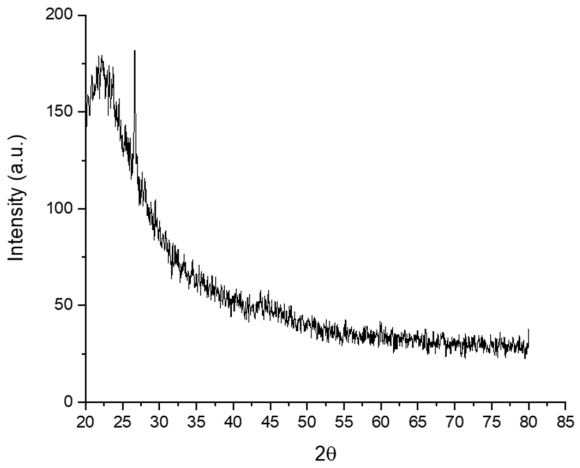

Figure 4. XRD spectrum of RHA.

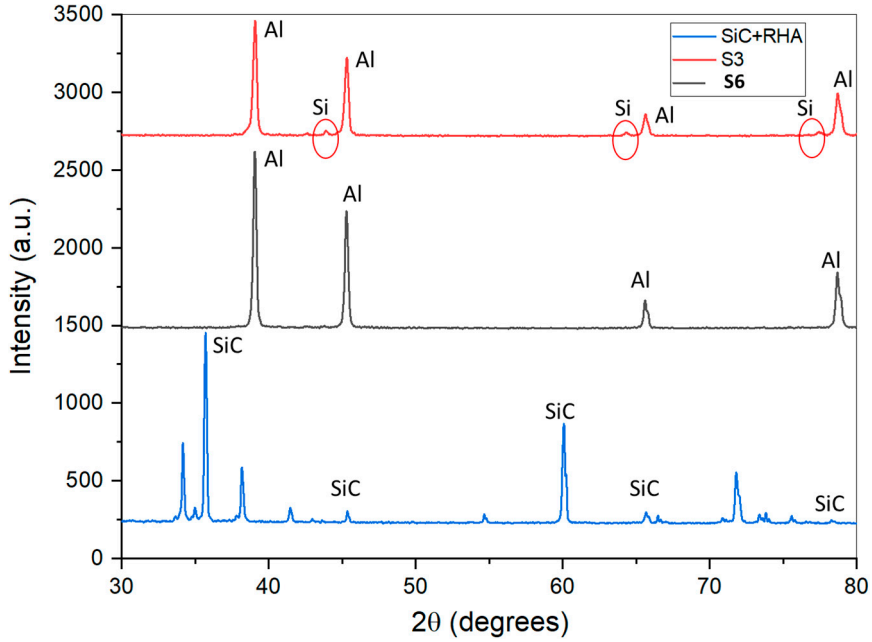

Figure 5. XRD spectra of pure AA8011 alloy (S6), HMMC with 4SiC/2.5RHA (S3), and RHA+SiC powder mix.

3.3. Hardness

The variation in Rockwell hardness across different samples is shown in Figure 6. It was clearly evidenced that the reinforcement had a positive effect on the hardness. The samples with the highest percentage by weight of reinforcement were the hardest, while the original Al alloy displayed the lowest hardness. The effect of RHA when added to the pure alloy (S5) is not quite clear, as there was no significant difference between S5 and S6. The slight increase in hardness can be explained by the fact that the RHA dissolved in the liquid AA8011 alloy and caused chemical alloying and second-phase precipitation. However, this explanation needs to be interpreted with caution.

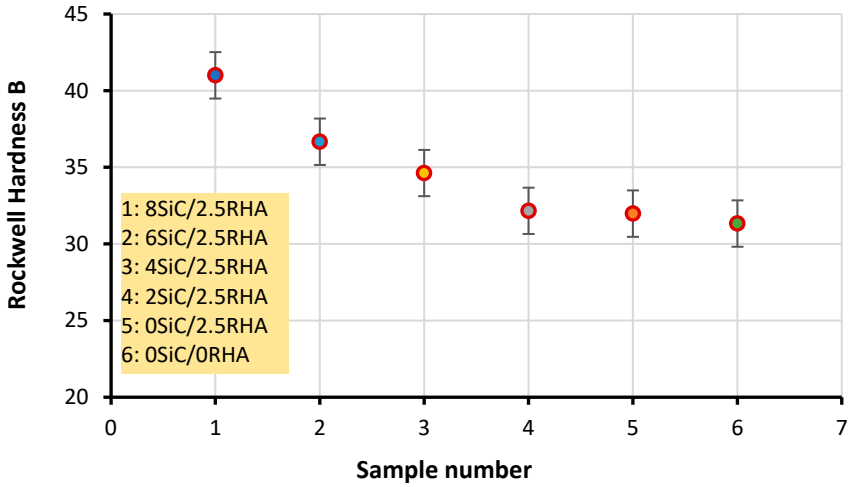

Figure 6. Variation in hardness, with sample numbers.

3.4. Wear Tests Results

3.4.1. Coefficient of Friction

The plot of COF against the sliding distance, in meters, at 200 °C is shown in Figure 7. It was noticed that, for the first few rotations, the COF rose exponentially to a peak value due to the higher friction force. This explains the opposing behaviour of dry friction and

transition from static to kinematic friction. After this transition, COF attained a lower asymptotic value, possibly due to the steady state being reached. For Sample 5, the COF peak value decreased and the asymptotic value at the steady state increased compared to that of Sample S6. The former might be attributed to the lubrication effect of RHA, and the latter might have resulted from the RHA's abrasiveness. However, COF significantly increased with the amount of SiC particles, possibly due to its abrasive effect compared to the samples (S5 and S6) without any SiC. However, it should be noted that, compared to the pure alloy, the 8SiC/2.5RHA (S1) reinforced composite showed significantly higher COF.

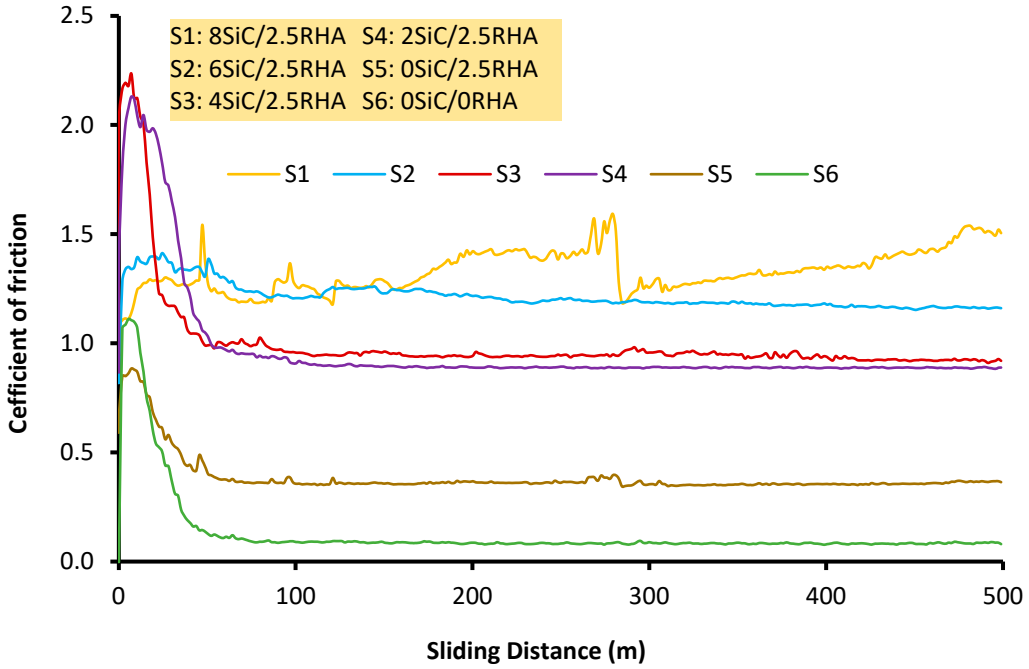

Figure 7. Variation in COF with the sliding distance at 200 °C.

The values of the coefficient of friction, as reported by researchers for AMMCs, usually fall between 0.25–0.65 depending upon testing parameters such as load, speed, etc. [31–34]. In this case, however, the COF values for samples S1, S2 and S3 were considerably higher than these values. This could be explained by the high amount of Si reinforcement added to the base alloy and the Si coming from both of the abrasive particles. RHA could add to this extraordinary high coefficient of friction.

3.4.2. Wear Volume Loss and Specific Wear

Figure 8 depicts the variation in the loss of material with composition and varying temperatures. The volume loss was measured in all the samples after the same sliding distance of 500 m. This was calculated by carefully weighing each sample before and after the wear test, then dividing it by the average density of the HMMC. The volumetric wear is usually calculated as mm^3 per meter, and it also decreases with increases in the reinforcement [33,34]. It can clearly be observed that the eroded volume increases almost linearly with decreasing reinforcement. As expected, the material loss was at its maximum in the sample without any reinforcement. This implies that addition of abrasive particles of SiC and RHA improves the wear behaviour of the HMMCs. The addition of RHA reduced the wear volume to a certain extent when compared to the pure alloy. The HMMC with 8 wt.% SiC showed the lowest wear volume due to the improvement in hardness compared to the mixed powder. Another factor that affects the wear is the operating temperature. At higher temperatures, the composite suffers severe volume loss, which may be due to

delamination. This is because higher temperatures render the alloys soft, and the wear behaviour transitions from adhesive to delamination.

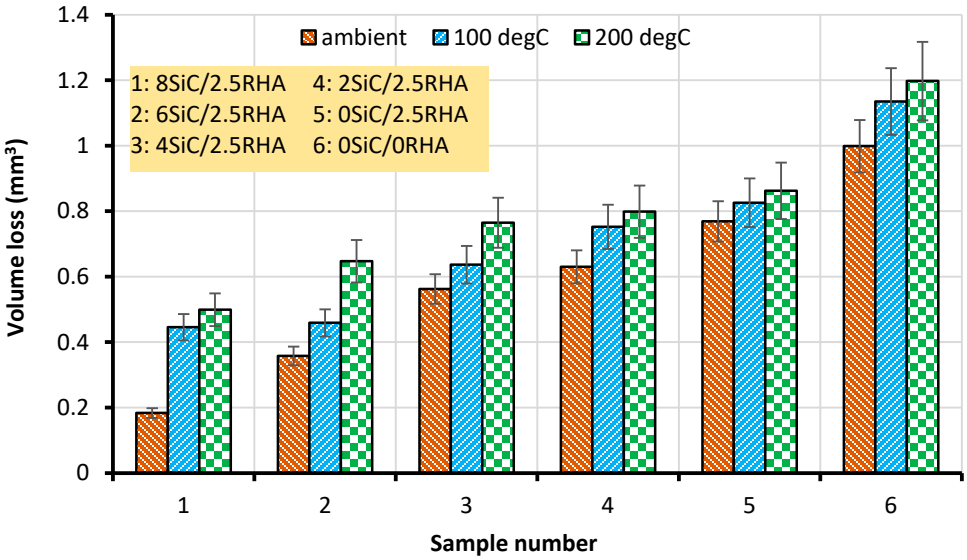

Figure 8. Variation in the volume loss of different samples at different ambient temperatures.

Specific wear was calculated as the total amount of worn pin material (µm) over the total sliding distance (m). Figure 9 shows a plot of the variation in specific wear (µm/m), with composition and operating temperatures. The wear increased with increasing temperatures and with decreasing percentages of reinforcement. It can be inferred from the plot that at 200°C, for the composite with no reinforcement, the wear was most severe, while the best tribological performance was exhibited by the composite with the highest reinforcement at an ambient temperature. With the addition of only RHA, the specific wear did not decrease significantly when compared to the non-reinforced Al alloy. However, the HMMC with 8.0 wt.% SiC reduced the specific wear by nearly a factor of 20 at 200 °C.

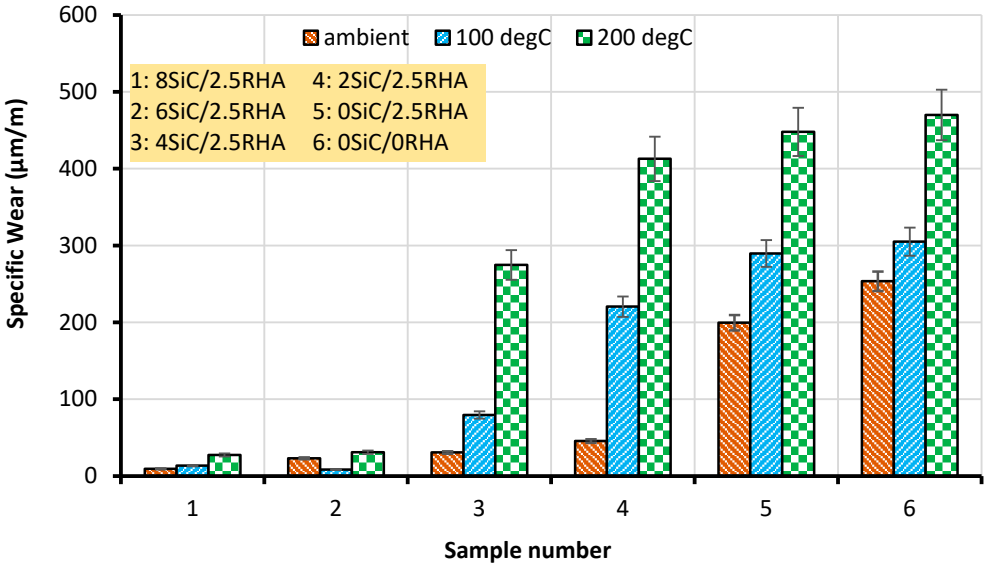

Figure 9. Variation in specific wear at different temperatures.

3.4.3. Worn Surface of the Disc

For studying wear in tribological systems, a tribometer is used. A tribometer is a pair of a pin and a disc, where the pin is a softer material sliding over the much harder disc.

Thus, it is important to analyse the surfaces of both the pin and the disc to gain better insight into the wear process. The wear track of the disc was observed under an optical microscope at a magnification of ×50, and the images are shown in Figure 10. The wear tracks show that fine grooves were developed on the surface of the disc. The losses of material from the disc surface are marked by red enclosures, and the sliding directions are marked with red lines. In Figure 10c, some small particles of the pin can be seen inside the red oval. This can be due to the erosion of the pin surface at a high temperature of 200 °C. The delamination of the pin surfaces may have caused the Al particles to scatter on the wear track, and high temperature could have caused the welding of the pin particles on the wear track due to the softening of the pin material. However, the presence of the pin material on the wear track cannot be confirmed by EDX analysis due to the large size of the disk. However, the wear of the pin track was much less severe than that observed on the worn pin surfaces. This was because the disc material was much harder than the pin material.

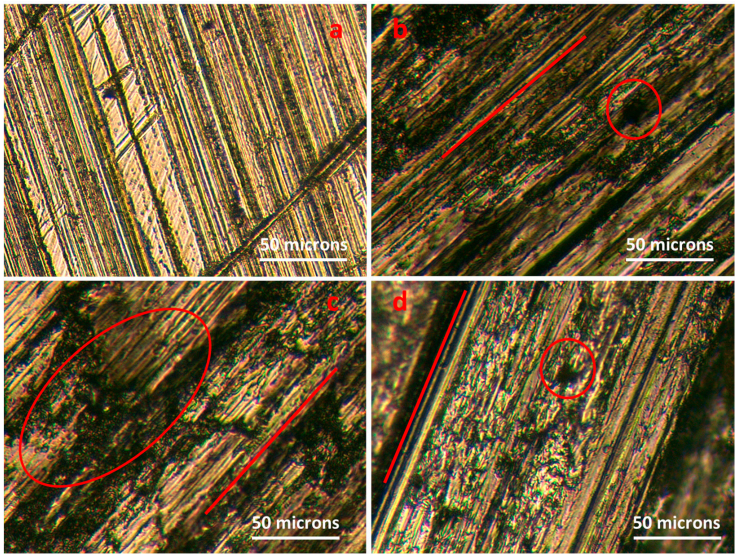

Figure 10. Optical microscopic images of the wear track of the disc at ×50 when testing the wear of 8SiC/2.5RHA at 200 °C: (**a**) ground disc surface before wear; images of the wear track at (**b**) position 1, (**c**) position 2, and (**d**) position 3.

3.4.4. Worn Surface Morphology of the Pin

The worn surfaces of the pins tested at 200 °C are shown in Figure 11. The maximum loss of material due to wear was observed in the unreinforced AA-8011, and minimum wear was observed in the 8SiC/2.5RHA HMMC. This result is aligned with the improvement in the hardness of the samples which was observed with greater reinforcement. Some interesting findings regarding the wear surface morphology are discussed below:

a. In the samples with higher reinforcement, larger amounts of SiC inclusions could be observed, while the wear mechanisms were mostly adhesive and abrasive, with almost negligible delamination and wear debris. It can further be stated that strong adhesion and intermetallic bonding between the ductile AA8011 and hard SiC particles were responsible for bearing the load and enhancing hardness, restricting the wear of the surface of the composite [35].
b. As the amount of reinforcement increased, the wear behaviour can possibly transition from slightly adhesive to abrasive, due to the presence of more abrasive SiC particles in the metal matrix. Overall, the predominant wear mechanism was abrasive in the HMMCs. Similar observations have been reported by other researchers in the literature [36–38].
c. Another important observation could be the presence of small, almost circular bright spots scattered on the worn surface (marked with green circles), identified thanks

to closer inspection. These could possibly be explained as wear debris, which was also reported by Mazahari and Shabani. They reported that this debris is found due to the propagation of cracks perpendicular to the sliding direction in the Al alloys with lower reinforcement [39]. The presence of larger amounts of this debris in the samples with less and no reinforcement indicates that, most probably, the material was being removed at a rate which did not allow for oxide film to be formed on the softer metal matrix surface [19]. In summary, the addition of RHA and SiC to AA8011 metal composites improved the wear resistance by affecting multiple wear mechanisms, including abrasion and adhesion.

The hard and abrasive particles of SiC act as reinforcements and increase the hardness and wear resistance of the composite material. Further, the abrasive particles could form a protective layer on the surface of the composite material, which can prevent adhesion between the mating surfaces and reduce the amount of wear.

d. In the cases of 0SiC/2.5RHA and 0SiC/0RHA, plastic deformation and subsequent delamination were observed due to the comparatively softer nature of the materials. It was most severe in the latter case, as it was unreinforced and more prone to delamination at higher temperatures. This indicated that there was a minor effect of RHA on the reduction in delamination wear. This observation strongly supported the results obtained regarding the increased loss of weight in the unreinforced alloy [11].

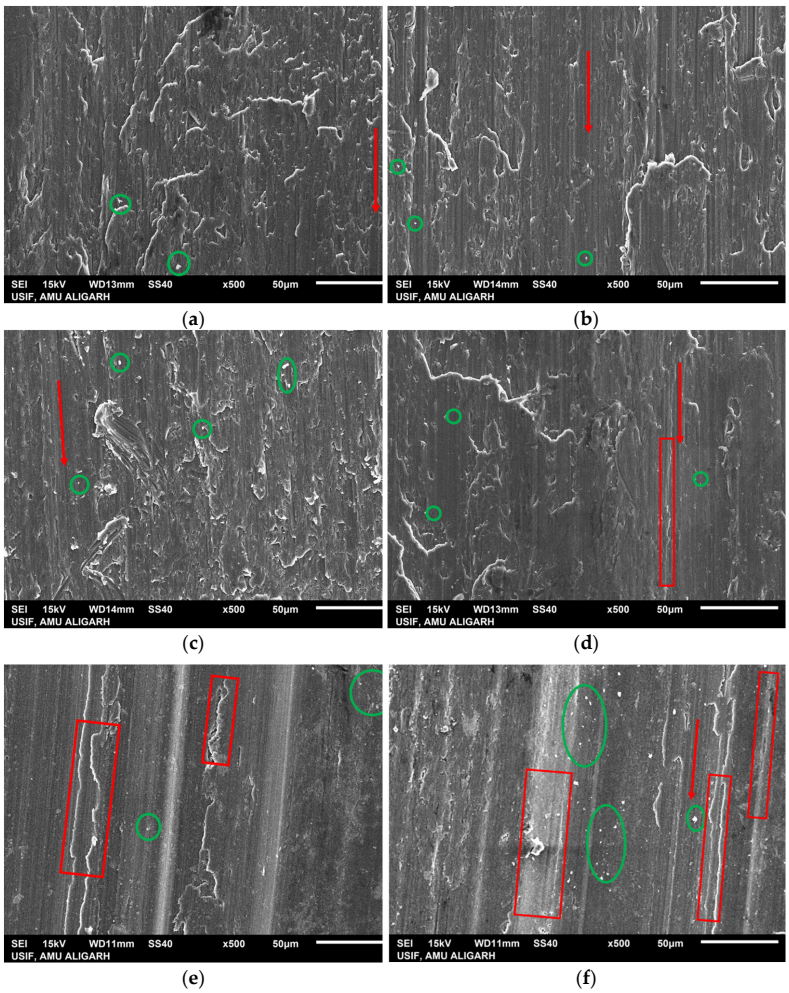

Figure 11. SEM micrographs of worn pin surfaces at 200 °C. (**a**) 8SiC/2.5RHA, (**b**) 6SiC/2.5RHA, (**c**) 4SiC/2.5RHA, (**d**) 2SiC/2.5RHA, (**e**) 0SiC/2.5RHA, and (**f**) 0SiC/0RHA, at ×500 magnification. Sliding direction, debris, and delamination are highlighted by red arrows, green circles, and red rectangles, respectively.

The results of the wear behaviour under different operating temperatures were also consistent with the previous research conducted in this field. However, at any fixed temperature, the best performance was exhibited by the composite with the highest SiC/RHA reinforcement. Therefore, the reinforced composites could be a better option for use in high-temperature applications. As the use of AA8011 alloys is prevalent in the automotive sector, the use of reinforced AA8011 alloys will provide a suitable option for parts for which relative movement is involved.

4. Conclusions

Hybrid metal matrix composites of AA8011 Al alloys were manufactured using the stir casting technique, with a fixed content (2.5 wt.%) of RHA and varying percentage of SiC (0, 2, 4, 6, 8 wt.%). From the microstructural, hardness, and wear testing results, the following conclusions can be drawn:

RHA particles showed bimodal particle distribution with smaller particles (7 μm to 15.6 μm) and larger particles (46.8 μm to 156.2 μm) with amorphous structures. The RHA particles completely dissolved in the metal matrix to form a second phase of Si in Al, which was spread homogenously throughout the matrix. From the surface morphology of the cast composites, a distribution of large groups or pockets of SiC particles throughout the AA8011 matrix was evident.

The effect of Al alloy reinforcement with SiC+RHA on the hardness and wear behaviour was consistent, with different weight percentages used in the synthesis of HMMCs. Although there was no significant difference in hardness observed after adding RHA in the aluminium alloy, SiC addition significantly increased the composite hardness. The tribological performance increased almost linearly with the level of reinforcement. The best performance was exhibited by the 8 wt.% SiC+RHA composite, while the lowest resistance to wear was exhibited by the pure cast Al alloy. The results of the wear behaviour under different operating temperatures were also consistent, while the wear properties degraded with increasing temperatures, irrespective of the amount of reinforcement. However, at a fixed temperature, the best performance was exhibited by the composite with the highest SiC/RHA reinforcement. It should also be noted that COF increased with the addition of both RHA and SiC particles, although the latter displayed a significant effect. Therefore, hybrid composites could be a better option for use as alternatives to cast iron in automotive engine components.

Author Contributions: Conceptualisation, S.M., J.H., P.M. and Q.M.; methodology, S.M. and J.H.; validation, J.H.; formal analysis, S.M., J.H., P.M. and Q.M.; investigation, S.M. and Q.M.; resources, Q.M.; data curation, S.M.; writing—original draft preparation, S.M.; writing—review and editing, S.M., J.H., P.M. and Q.M.; visualisation, S.M.; supervision, P.M. and J.H.; project administration, Q.M. All authors have read and agreed to the published version of the manuscript.

Funding: This research received no external funding.

Institutional Review Board Statement: Not applicable.

Informed Consent Statement: Not applicable.

Data Availability Statement: The data presented in this study are available within the article.

Acknowledgments: The authors sincerely acknowledge the facility provided by Delhi Technological University (D.T.U.), New Delhi, India, to prepare the stir-cast samples. The authors also acknowledge the facilities provided by Aligarh Muslim University (AMU) for the characterisation of the samples. We would like to thank Unais Sait (Free University of Bozen-Bolzano, Italy) for helping us to structure this article.

Conflicts of Interest: The authors declare no conflict of interest.

References

1. Ngo, T.-D. (Ed.). Introduction to Composite Materials. In *Composite and Nanocomposite Materials*; IntechOpen: Rijeka, Croatia, 2020.
2. Verma, A.; Chauhan, S.S.; Dwivedi, S.P. Review Paper on Thermal Expansion and Tribological Behavior of Composite Materials. *Mater. Today Proc.* **2023**, *79*, 235–246. [CrossRef]
3. Mavhungu, S.; Akinlabi, E.; Onitiri, M.; Varachia, F. Aluminum Matrix Composites for Industrial Use: Advances and Trends. *Procedia Manuf.* **2017**, *7*, 178–182. [CrossRef]
4. Miteva, A.; Petrova, A.; Stefanov, G. Surface Oxidation of Al-Si Alloys at Elevated Temperatures. *Appl. Eng. Lett. J. Eng. Appl. Sci.* **2021**, *6*, 105–110. [CrossRef]
5. Reddy, K.S.K.; Lekha, B.C.; Sakshi, K.U.; Chouhan, M.S.; Karthikeyan, R.; Aparna, S. Effect of Different Reinforcements on Aluminium Composite Properties—A Review. *Mater. Today Proc.* **2022**, *62*, 3963–3967. [CrossRef]
6. Yigezu, B.S.; Mahapatra, M.M.; Jha, P.K. Influence of Reinforcement Type on Microstructure, Hardness, and Tensile Properties of an Aluminum Alloy Metal Matrix Composite. *J. Miner. Mater. Charact. Eng.* **2013**, *1*, 33948.
7. Singh, K.M.; Chauhan, A.K. Fabrication, Characterization, and Impact of Heat Treatment on Sliding Wear Behaviour of Aluminium Metal Matrix Composites Reinforced with B4C. *Adv. Mater. Sci. Eng.* **2021**, *2021*, 1–9. [CrossRef]
8. Singh, J. Fabrication Characteristics and Tribological Behavior of Al/SiC/Gr Hybrid Aluminum Matrix Composites: A Review. *Friction* **2016**, *4*, 191–207. [CrossRef]
9. Chaudhari, A.D.; Danej, A.A.; Nirbhavane, P.S.; Shinde, S.S.; Pawar, S.Y. Wear Behaviour Analysis of Silicon Carbide Based Aluminium Metal Matrix Composites. *Int. Res. J. Eng. Technol.* **2020**, *7*, 5754–5759.
10. Daniel, A.A.; Murugesan, S.; Sukkasamy, S. Others Dry Sliding Wear Behaviour of Aluminium 5059/SiC/MoS_2 Hybrid Metal Matrix Composites. *Mater. Res.* **2017**, *20*, 1697–1706. [CrossRef]
11. Subramaniam, B.; Natarajan, B.; Kaliyaperumal, B.; Chelladurai, S.J.S. Wear Behaviour of Aluminium 7075—Boron Carbide-Coconut Shell Fly Ash Reinforced Hybrid Metal Matrix Composites. *Mater. Res. Express* **2019**, *6*, 1065d3. [CrossRef]
12. David Raja Selvam, J.; Dinaharan, I.; Mashinini, P. High Temperature Sliding Wear Behavior of AA6061/Fly Ash Aluminum Matrix Composites Prepared Using Compocasting Process. *Tribol.-Mater. Surf. Interfaces* **2017**, *11*, 39–46. [CrossRef]
13. Aghaie-Khafri, M. Formability of AA8011 Aluminum Alloy Sheet in Homogenized and Unhomogenized Conditions. *J. Mater. Sci.* **2004**, *39*, 6467–6472. [CrossRef]
14. Fayomi, J.; Popoola, A.; Popoola, O.; Fayomi, O.; Ajenifuja, E. Response Evaluation of AA8011 with Nano ZrB_2 Inclusion for Multifunctional Applications: Considering Its Thermal, Electrical, and Corrosion Properties. *J. Alloys Compd.* **2021**, *853*, 157197. [CrossRef]
15. Karthikeyan, A.; Nallusamy, S. Experimental Analysis on Sliding Wear Behaviour of Aluminium-6063 with SiC Particulate Composites. *Int. J. Eng. Res. Afr.* **2017**, *31*, 36–43. [CrossRef]
16. Benal, M.M.; Shivanand, H. Effects of Reinforcements Content and Ageing Durations on Wear Characteristics of Al (6061) Based Hybrid Composites. *Wear* **2007**, *262*, 759–763. [CrossRef]
17. Hillary, J.J.M.; Ramamoorthi, R.; Chelladurai, S.J.S. Dry Sliding Wear Behaviour of Al6061–5% SiC—TiB_2 Hybrid Metal Matrix Composites Synthesized by Stir Casting Process. *Mater. Res. Express* **2020**, *7*, 126519. [CrossRef]
18. Karthikkumar, C.; Baranirajan, R.; Premnauth, I.; Manimaran, P. Investigations on Mechanical Properties of Al 8011 Reinforced with Micro B4C/Red Mud by Stir Casting Method. *Int. J. Eng. Res. Gen. Sci.* **2016**, *4*, 405.
19. Pramanik, A. Effects of Reinforcement on Wear Resistance of Aluminum Matrix Composites. *Trans. Nonferrous Met. Soc. China* **2016**, *26*, 348–358. [CrossRef]
20. Zhu, H.; Jar, C.; Song, J.; Zhao, J.; Li, J.; Xie, Z. High Temperature Dry Sliding Friction and Wear Behavior of Aluminum Matrix Composites (Al_3Zr + α-Al_2O_3)/Al. *Tribol. Int.* **2012**, *48*, 78–86. [CrossRef]
21. Al-Salihi, H.A.; Mahmood, A.A.; Alalkawi, H.J. Mechanical and Wear Behavior of AA7075 Aluminum Matrix Composites Reinforced by Al_2O_3 Nanoparticles. *Nanocomposites* **2019**, *5*, 67–73. [CrossRef]
22. Hossain, S.S.; Mathur, L.; Roy, P. Rice Husk/Rice Husk Ash as an Alternative Source of Silica in Ceramics: A Review. *J. Asian Ceram. Soc.* **2018**, *6*, 299–313. [CrossRef]
23. Bulei, C.; Stojanovic, B.; Utu, D. Developments of Discontinuously Reinforced Aluminium Matrix Composites: Solving the Needs for the Matrix. *Proc. J. Phys. Conf. Ser.* **2022**, *2212*, 012029. [CrossRef]
24. Bhushan, B. *Introduction to Tribology*; John Wiley & Sons: Hoboken, NJ, USA, 2013.
25. *ASTM G99-17 2017*; Standard Test Method for Wear Testing with a Pin-on-Disk Apparatus. ASTM International: West Conshohocken, PA, USA, 2017.
26. García-Miranda, J.S.; Aguilera-Camacho, L.D.; Hernández-Sierra, M.T.; Moreno, K.J. A Comparative Analysis of the Lubricating Performance of an Eco-Friendly Lubricant vs Mineral Oil in a Metallic System. *Coatings* **2023**, *13*, 1314. [CrossRef]
27. Karthikeyan, A.; Jinu, G. Investigation on Mechanical and Corrosion Behaviour of AA8011 Reinforced with TiC and Graphite Hybrid Composites. *Mater. Res. Express* **2019**, *6*, 1065b5. [CrossRef]
28. Liou, T.-H.; Chang, F.-W.; Lo, J.-J. Pyrolysis Kinetics of Acid-Leached Rice Husk. *Ind. Eng. Chem. Res.* **1997**, *36*, 568–573. [CrossRef]
29. Azizi, S.N.; Yousefpour, M. Spectroscopic Studies of Different Kind of Rice Husk Samples Grown in North of Iran and the Extracted Silica by Using XRD, XRF, IR, AA and NMR Techniques. *Eurasian J. Anal. Chem.* **2008**, *3*.

30. Arif, S.; Jamil, B.; Shaikh, M.B.N.; Aziz, T.; Ansari, A.H.; Khan, M. Characterization of Surface Morphology, Wear Performance and Modelling of Graphite Reinforced Aluminium Hybrid Composites. *Eng. Sci. Technol. Int. J.* **2020**, *23*, 674–690. [CrossRef]
31. Mistry, J.M.; Gohil, P.P. An Overview of Diversified Reinforcement on Aluminum Metal Matrix Composites: Tribological Aspects. *Proc. Inst. Mech. Eng. Part J J. Eng. Tribol.* **2017**, *231*, 399–421. [CrossRef]
32. Padmavathi, K.; Ramakrishnan, R. Tribological Behaviour of Aluminium Hybrid Metal Matrix Composite. *Procedia Eng.* **2014**, *97*, 660–667. [CrossRef]
33. Lakshmikanthan, A.; Angadi, S.; Malik, V.; Saxena, K.K.; Prakash, C.; Dixit, S.; Mohammed, K.A. Mechanical and Tribological Properties of Aluminum-Based Metal-Matrix Composites. *Materials* **2022**, *15*, 6111. [CrossRef]
34. Naik, M.H.; Manjunath, L.; Koti, V.; Lakshmikanthan, A.; Koppad, P.G.; Kumaran, S.P. Al/Graphene/CNT Hybrid Composites: Hardness and Sliding Wear Studies. *FME Trans.* **2021**, *49*, 414–421. [CrossRef]
35. Fayomi, J.; Popoola, A.P.I.; Popoola, O.M.; Oladijo, O.P.; Fayomi, O.S.I. Tribological and Microstructural Investigation of Hybrid AA8011/ZrB2-Si3N4 Nanomaterials for Service Life Improvement. *Results Phys.* **2019**, *14*, 102469. [CrossRef]
36. Sharma, A.; Belokar, R.; Kumar, S. Dry Sliding Wear Characterization of Red Mud Reinforced Aluminium Composite. *J. Braz. Soc. Mech. Sci. Eng.* **2018**, *40*, 1–12. [CrossRef]
37. Thirumalai Kumaran, S.; Uthayakumar, M. Investigation on the Dry Sliding Friction and Wear Behavior of AA6351-SiC-B4C Hybrid Metal Matrix Composites. *Proc. Inst. Mech. Eng. Part J J. Eng. Tribol.* **2014**, *228*, 332–338. [CrossRef]
38. Sahin, Y.; Murphy, S. The Effect of Sliding Speed and Microstructure on the Dry Wear Properties of Metal-Matrix Composites. *Wear* **1998**, *214*, 98–106. [CrossRef]
39. Mazahery, A.; Shabani, M.O. Ascending Order of Enhancement in Sliding Wear Behavior and Tensile Strength of the Compocast Aluminum Matrix Composites. *Trans. Indian Inst. Met.* **2013**, *66*, 171–176. [CrossRef]